


An Immunologically Modified Nanosystem Based on Noncovalent Binding Between Single-Walled Carbon Nanotubes and Glycated Chitosan

Technology in Cancer Research & Treatment
Volume 17: 1-8
© The Author(s) 2018
Article reuse guidelines:
sagepub.com/journals-permissions
DOI: 10.1177/1533033818802313
journals.sagepub.com/home/tct


Leton Chandra Saha, PhD¹, Okhil Kumar Nag, PhD²,
Austin Doughty, BA³, Hong Liu, PhD⁴, and Wei R. Chen, PhD³ 

Abstract

Functionalized single-walled carbon nanotubes are currently being explored as novel delivery vehicles for proteins and therapeutic agents to treat various diseases. In order to maximize treatment efficacy, a strong binding between single-walled carbon nanotubes and their functionalized molecules is necessary. Glycated chitosan, a polymer with potent immunostimulatory properties for cancer treatment, has been used as a surfactant of single-walled carbon nanotubes to form an immunologically modified nanosystem for biomedical applications. In this study, we investigated the binding characteristics of single-walled carbon nanotube and glycated chitosan using molecular dynamics simulations. The mean square displacement, radius of gyration, interaction energy, and radial distribution function of the single-walled carbon nanotube-glycated chitosan system were analyzed. The results from the simulations demonstrated that glycated chitosan was bound to single-walled carbon nanotubes by a strong, noncovalent interaction. The stability of glycated chitosan on the single-walled carbon nanotubes surface was enhanced by the length of glycated chitosan, and the binding energy of the 2 molecules was closely related to the diameter and chirality of single-walled carbon nanotubes, with the most stable single-walled carbon nanotube-glycated chitosan system being formed by the combination of long polymer, large single-walled carbon nanotube, and armchair single-walled carbon nanotube. The understanding of the interactions between single-walled carbon nanotube and glycated chitosan and the structure of single-walled carbon nanotube-glycated chitosan allows the modifications of the novel nanosystem for disease diagnostics and therapeutics.

Keywords

carbon nanotubes, glycated chitosan, molecular dynamics simulation, interaction energy, noncovalent binding

Abbreviations

BB, backbone; GC, glycated chitosan; LIT, laser immunotherapy; MD, molecular dynamics; MSD, mean square displacement; NIR, near-infrared; RDFs, radial distribution functions; RUs, repeating units; SC, sidechain; SWNTs, single-walled carbon nanotubes.

Received: October 25, 2017; Revised: July 28, 2018; Accepted: August 27, 2018.

Introduction

Single-walled carbon nanotubes (SWNTs) were developed more than 2 decades ago and have been utilized to advance research development in many fields.¹⁻³ Single-walled carbon nanotubes have shown great promise in medical applications due to their strong optical absorbance in the near-infrared (NIR) region,^{4,5} their ability to cross cellular membranes without eliciting cytotoxicity,^{6,7} and their capability as delivery vehicles for therapeutic agents and proteins.⁸⁻¹⁰ Single-walled carbon nanotubes can affect immune systems with desired

¹ Inamori Frontier Research Center, Kyushu University, Fukuoka, Japan

² Center for Bio/Molecular Science and Engineering, Naval Research Laboratory, Washington, DC, USA

³ Biophotonics Research Laboratory, Center for Interdisciplinary Biomedical Education and Research, College of Mathematics and Science, University of Central Oklahoma, Edmond, OK, USA

⁴ Center for Bioengineering and School of Electrical and Computer Engineering, University of Oklahoma, Norman, OK, USA

Corresponding Author:

Wei R. Chen, PhD, Biophotonics Research Laboratory, Center for Interdisciplinary Biomedical Education and Research, College of Mathematics and Science, University of Central Oklahoma, Edmond, OK 73034, USA.
Email: wchen@uco.edu



functionalization for effective targeting of cancer cells.¹¹⁻¹⁴ Other carbon nanomaterials such as graphene oxide have been reported to serve as immune stimulators.^{14,15} The immunological effect of nanomaterials has attracted more and more attention.

Single-walled carbon nanotubes are not independently soluble in aqueous media and thus require a surfactant.¹⁶ Glycated chitosan (GC), a water-soluble derivative of chitosan, is a potent immunostimulant that can act as a surfactant for SWNT while maintaining its immunostimulatory properties.^{17,18} Our previous work demonstrated that the SWNT-GC system is not toxic *in vitro* and *in vivo* by itself while imposing stimulatory effect on immune cells.^{17,18} Single-walled carbon nanotube-GC was used in conjunction with NIR laser irradiation, a process called laser immunotherapy (LIT), to treat metastatic cancers.^{17,19} Single-walled carbon nanotube-GC is a particularly useful nanosystem for LIT, as it acts as a photothermal transducer to enhance the local selectivity of light absorption and as an immunostimulant to enhance antitumor immune response following laser irradiation.¹⁷ The binding characteristics of the SWNT-GC system are currently unknown. This presents an issue, as superfluous GC in the media could decrease the selectivity of light absorption and thus the efficacy of LIT treatment. Several challenges lie in understanding the binding between SWNT and GC. Properties of SWNT, such as its length, diameter, and chirality, can affect the SWNT-GC binding.¹⁶ Furthermore, the length of GC in its polymer form varies, depending on its synthesis process, and it can also affect the SWNT-GC binding.

It is challenging to determine the SWNT-GC binding characteristics experimentally due to the different properties of GC and SWNT. For one, it is very difficult to control the number of monomers that form the GC polymer during GC synthesis.²⁰ Additionally, SWNTs can have different chiralities and diameters to affect the interaction energy and gyration characteristics of the SWNT-GC system.²¹⁻²³ As a result, a reliable simulation is needed to determine the SWNT-GC binding characteristics.

Molecular dynamics (MD) simulations have been employed to investigate SWNT and polymer interactions.²⁴⁻²⁷ However, the interactions between SWNT and GC have not been investigated using MD. In this study, we focused on the relationships between the SWNT-GC binding and the length of GC. We also investigated GC morphology based on SWNT diameter, length, and chirality. The understanding of the dynamic and structural properties of SWNT-GC can help further modifications of SWNT-GC for biomedical applications.

Methods and Materials

Molecular dynamics simulations were performed using the DL_POLY 2.20.²⁸ For all calculations, the initial temperature was set at 300 K. A cubic simulation box with an edge length of 300.0 Å was used, and periodic boundary conditions were imposed. For constant number, volume, and temperature simulations, we used the Nose-Hoover thermostat.²⁹ The GC

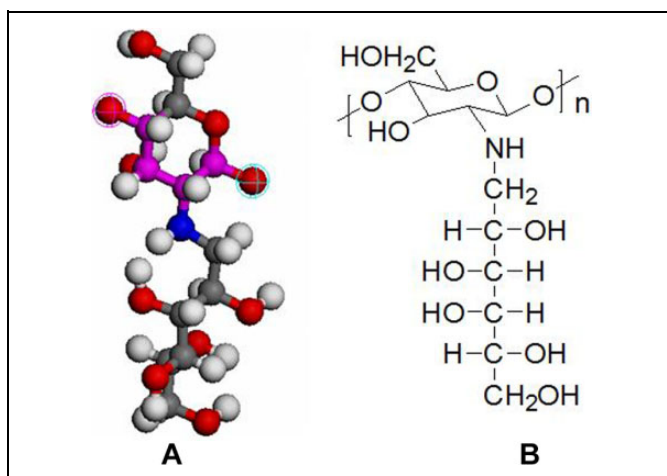


Figure 1. A monomer of GC molecule used in this study. A, A ball-and-stick model of GC, with C, N, O, and H atoms are grey, blue, red, and white, respectively. The atoms drawn in pink show the carbon chain that forms the backbone of the polymer. B, The molecular structure of GC. GC indicates glycated chitosan.

polymer chain was initially placed alongside the SWNT at a distance of 20 Å. Each time step in the simulation was 1 fs, and the full simulation run time was 4 ns (an equilibration time of 0.5 ns and a production run time of 3.5 ns) to analyze structural and dynamic properties of GC polymers. With this time scale, the GC polymers were allowed to complete the wrapping process around the SWNT due to the attractive forces between the 2 molecules. To describe inter- and intramolecular interactions, we used DREIDING³⁰ potential (previously used by other researchers to study CNT-polymer systems³¹⁻³³). DREIDING potential function using harmonic form for bond stretching term, which is useful for simulating structures and dynamics of organic and biological molecules, was used. The potential function is described as,

$$E = \frac{K_b}{2}(R - R_0)^2 + \frac{K_\theta}{2}(\cos\theta - \cos\theta_0)^2 + V[1 + \cos(m\theta - \delta)] + C[1 - \cos\theta] + \left[\frac{A}{r_{ij}^{12}} - \frac{B}{r_{ij}^6} \right], \quad (1)$$

where K_b , K_θ , V and C are the bond, angle, torsional, and inversion constants, respectively, R_0 and θ_0 are the equilibrium bond lengths and angles, m is the multiplicity, and δ is the phase angle for torsional parameters. A and B are van der Waal's parameters and r_{ij} is the distance between the i th and j th atoms. In our simulations, the cutoff radius of every interaction potential were set to 10 Å.

The virtual GC and SWNT models were constructed using 2 programs, DL_POLY and visual molecular dynamics (VMD).³⁴ The following Figure 1 shows the chemical structure of GC used as a reference to construct its virtual structure. In most simulations, a GC polymer with 30 repeating units (RUs) had an end-to-end length of 126.4 Å, and a molecular weight of

Table 1. Repeating Units in the GC, and Diameters, Lengths, and Types of SWNT.

SWNT Chirality	SWNT Diameter	SWNT Length	RUs	Binding Energy, kcal/mol
(6,6) armchair	8.1	81.1	30	-342.47 (27.63)
(6,5) chiral	7.5	81.3	30	-222.10 (27.88)
(10,0) zigzag	7.83	81.8	30	-204.99 (26.10)
(9,9)	12.20	81.1	30	-310.28 (26.67)
(12,12)	16.27	81.1	30	-353.37 (31.61)
(15,15)	20.34	81.1	30	-423.73 (28.54)
(6,6)	8.1	110.68	30	-249.65 (33.32)
(6,6)	8.1	140.19	30	-271.78 (30.26)
(6,6)	8.1	169.71	30	-394.22 (29)
(6,6)	8.1	169.71	10	-104.10 (16.13)
(6,6)	8.1	169.71	20	-245.29 (19.84)
(6,6)	8.1	169.71	50	-549.94 (33)

Abbreviations: GC, glycosylated chitosan; RUs, repeated units; SWNT, single-walled carbon nanotube.

9316 Å was used. Table 1 provides the detailed information of the SWNTs and others GC polymers used in the simulations. For this study, the position of the atoms in the SWNT structure remained unchanged during simulation to reduce computational time. To avoid an unsaturated boundary effect, we added hydrogen atoms to the ends of the SWNTs.

Results

The Stability of GC on SWNT Surface

To understand the stability of the GC polymer on the surface of the SWNT, we calculated the mean square displacement (MSD) using the following equation:

$$MSD(t) = \langle |\mathbf{r}(t) - \mathbf{r}_0|^2 \rangle, \quad (2)$$

where $\mathbf{r}(t)$ is a vector-function of the position and \mathbf{r}_0 is the vector pointing to the initial position. First, the simulation was run for 0.5 ns to allow the formation of a stable binding between GC and SWNT molecules. Then, the simulation was continued for another 3.5 ns in order to analyze the difference in position over time. The SWNT used had a diameter and length of 8.1 Å and 170 Å, respectively, and the GC used was of 10, 20, 30, or 50 RU in length. The calculated MSDs are shown in Figure 2. The GC molecules with fewer RUs displayed a greater mobility on the SWNT surface than those with more RUs.

The Relationship Between GC Wrapping Behavior and SWNT Diameter

Figure 3 shows snapshots of the simulation. When a GC molecule (30 RUs) interacts with an SWNT, the arrangement of the monomers along the chain changed due to interactions with the surface of the SWNT. Figure 3A shows an armchair SWNT (9, 9) with a 12.20 Å diameter, where the GC had wrapped onto a linear shape around the SWNT surface. An armchair SWNT (12, 12) of 16.27 Å in diameter GC forms a helical type shape (Figure 3B). In Figure 3C, it is shown that GC loses its linear or

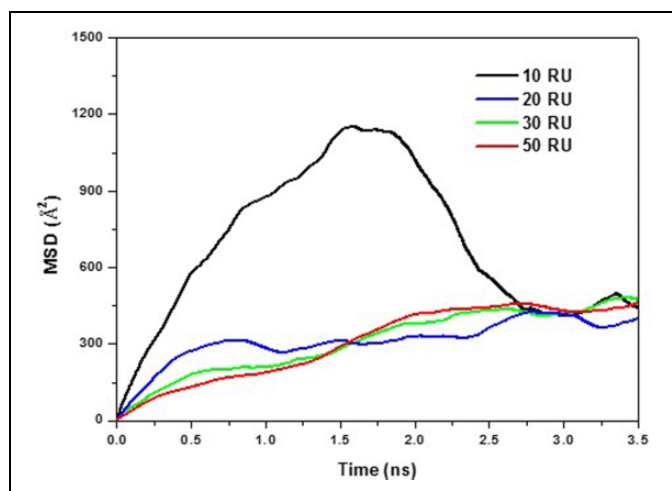


Figure 2. Mean square displacement (MSD) for GC traveling along an SWNT (6,6) surface. Four different sizes of GC with 10, 20, 30, and 50 repeating units (RUs) were used. GC with smaller RUs showed a greater MSD over time. GC indicates glycosylated chitosan; SWNT, single-walled carbon nanotube.

helical shape and attempt to fold when bound to (15, 15) SWNT of 20.34 Å. Our simulations indicate that GC geometry is influenced by diameter of SWNT.

To illustrate the overall size of the GC polymers on the SWNT surface, we calculated the radius of gyration (R_g) of the GC polymers using the following equation:

$$R_g^2 = \frac{1}{N} \sum_{i=1}^N (\mathbf{r}_i - \mathbf{r}_{cm})^2, \quad (3)$$

where \mathbf{r}_i and \mathbf{r}_{cm} indicate the position vector of each atom and the vector of the center-of-mass, respectively, and N is the number of atoms in the system. If R_g increases, it represents the expansion of GC polymer on SWNT surface. Figure 4 shows the time evolution of R_g for GC during the wrapping process of GC around SWNT (9, 9), SWNT (12, 12), and SWNT (15, 15), with diameters of 12.20, 16.27, and 20.34 Å,

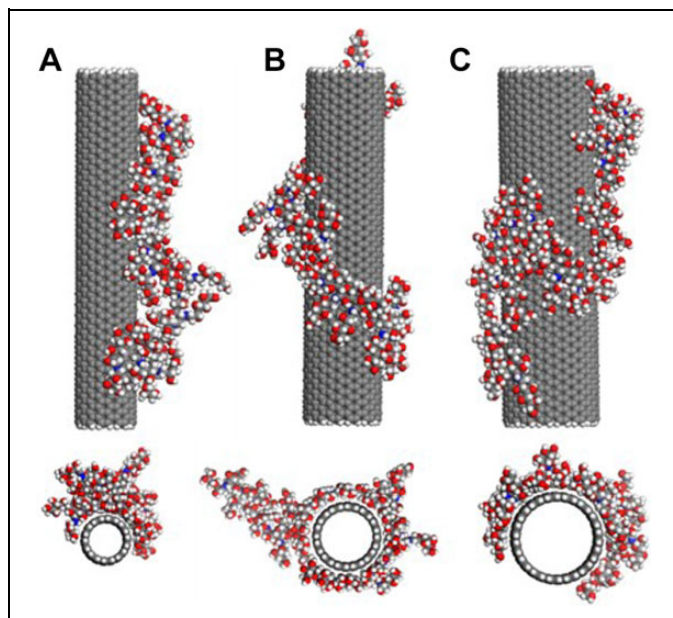


Figure 3. Simulation snapshots of the GC wrapped around SWNTs. Armchair SWNT, (9, 9), (12, 12), and (15, 15), with different diameters, (A) 12.20, (B) 16.27, (C) and 20.34 Å, respectively, were used. The Snapshots were taken at 3.5 ns. Drawn in grey, blue, red, and white are carbon, nitrogen, oxygen, and hydrogen atoms, respectively. GC indicates glycosylated chitosan; SWNT, single-walled carbon nanotube.

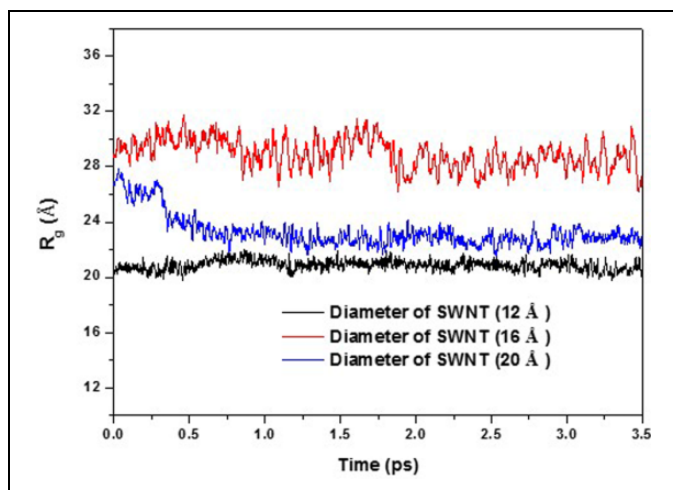


Figure 4. Radius of gyration of GC during interaction with SWNTs of different diameters as a function of time. SWNT of (9, 9), (12, 12), and (15, 15) with diameters of 12.20, 16.27 and 20.34 Å, respectively, were used. GC polymers were 30 RU. GC indicates glycosylated chitosan; SWNT, single-walled carbon nanotube; RU, repeating unit

respectively. With SWNT (9, 9), R_g was found to be 20.62 (0.36) Å. For SWNT (12, 12) and SWNT (15, 15), R_g was found to be 28.44 (0.99) and 22.95 (0.37) Å, respectively. R_g was calculated by taking the average value from 3.0 to 3.5 ns. While there is no clear pattern for the value of R_g in terms of the diameters, SWNT (12, 12) shows a relatively high R_g , this is

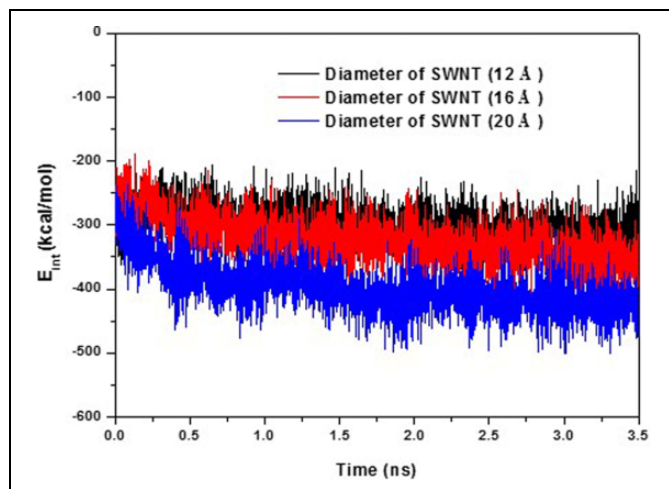


Figure 5. Interaction energies for SWNTs of different diameters with GC as a function of time. SWNT of (9, 9), (12, 12), and (15, 15) with diameters of 12.20, 16.27, and 20.34 Å, respectively, were used. GC polymers were 30 RU long. GC indicates glycosylated chitosan; RU, repeating unit; SWNT, single-walled carbon nanotube.

due to its shape, which is mainly effected by the wrapping process (see Figure 4).

We also calculated the interaction energy (E_{int}) between the SWNT and GC during the wrapping process by taking the configuration energy of the entire complex ($E_{complex}$), subtracting the configuration energies of the isolated SWNT (E_{SWNT}) and the isolated GC (E_{GC}):

$$E_{int} = E_{complex} - (E_{SWNT} + E_{GC}). \quad (4)$$

The interaction energies between GC polymer and SWNT with different diameters as a function of time is depicted in Figure 5. When GC wrapped into an SWNT of (15, 15), it had the strongest interaction with -423.73 (28.54) kcal/mol; when GC wrapped into an SWNT of (9, 9), it had the weakest interaction with -310.28 (26.67) kcal/mol; and when GC wrapped into an SWNT of (12, 12), it had a medium interaction energy of -353.37 (31.61) kcal/mol. Interaction energies were collected from the trajectory in the range of 3.0 to 3.5 ns and then averaged. We also presented their respective standard deviations.

The Impact of SWNT Chirality on GC's Wrapping Behavior

We investigated the wrapping characteristics of GC on SWNTs using 3 different chiralities: a zigzag SWNT (10, 0), an armchair SWNT (6, 6), and a chiral SWNT (6, 5). All SWNTs used had comparable length and diameter, 81.2 Å and 8.0 Å, respectively. Snapshots of the GC-SWNT interactions with different times are shown in Figure 6. Glycosylated chitosan wrapped around SWNTs of all chiralities in helical or semi-helical shapes indicating that SWNT chirality had little effect on the morphology of GC on the SWNT surface. We also calculated R_g for GC during the wrapping process around SWNT (6, 6), SWNT

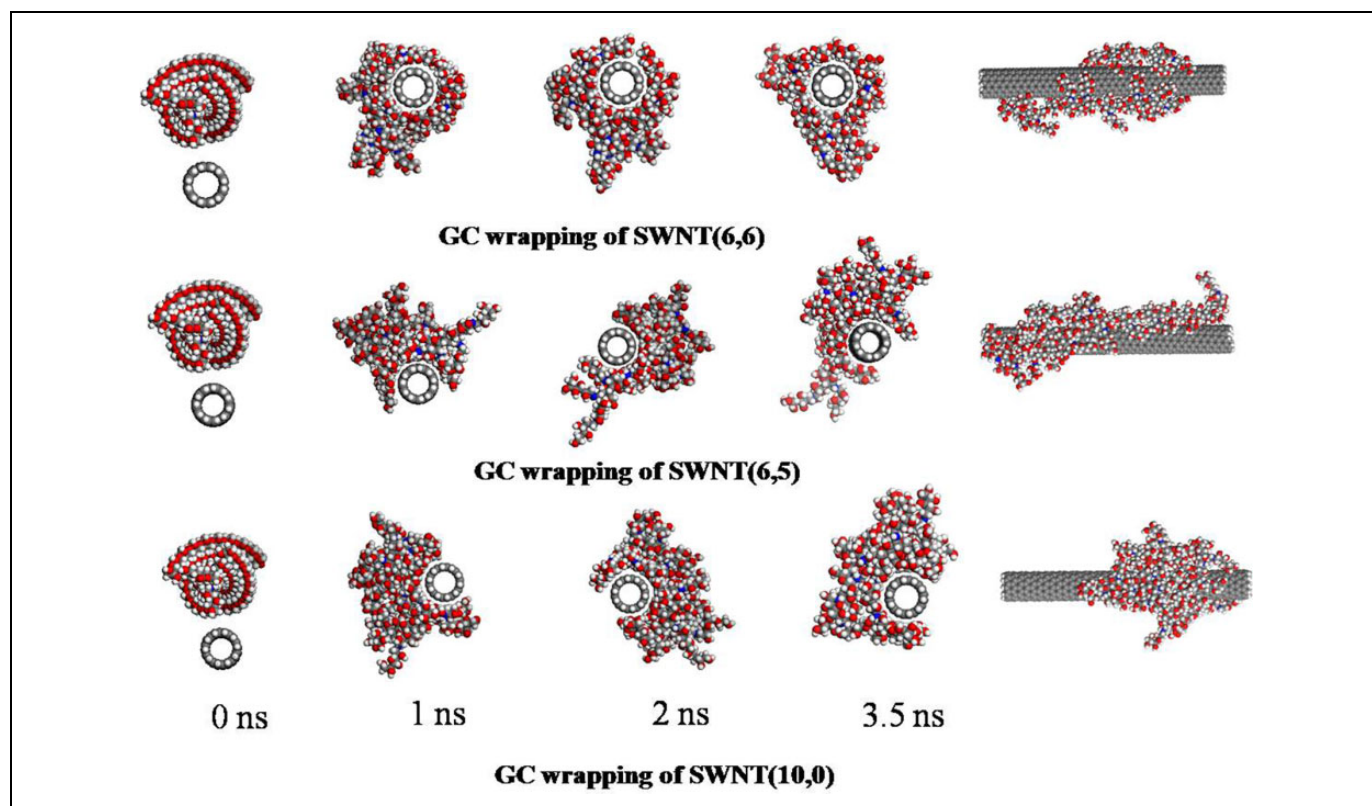


Figure 6. Simulation snapshots of GC wrapped around SWNTs of different chiralities: (A) SWNT of (6,6); (B) SWNT of (6, 5); and (C) SWNT of (10, 0). GC of 30 RU was used for all simulations. The snapshots were taken at 0, 1, 2, and 3.5 ns. Drawn in grey, blue, red, and white are carbon, nitrogen, oxygen, and hydrogen atoms, respectively. GC indicates glycated chitosan; RU, repeating unit; SWNT, single-walled carbon nanotube.

(6, 5), and SWNT (10, 0). These are $18.33 (0.23) \text{ \AA}$, $24.61 (0.26) \text{ \AA}$, and $14.93 (0.1) \text{ \AA}$, respectively. Among them, SWNT (10, 0) exhibits low R_g . Previously, we have explained this based on the shape of SWNT (see Figure 6).

The SWNT–GC interaction energy was also obtained for the 3 different chiralities using Equation 4. The interaction energies of the SWNT–GC systems are shown in Figure 7. The chiral SWNT (6, 5) and zigzag SWNT (10, 0) had significantly lower interaction energy, $-222.10 \pm 27.88 \text{ kcal/mol}$ and $-204.99 \pm 26.10 \text{ kcal/mol}$, respectively, than that of the armchair SWNT (6, 6), $-342.47 \pm 27.63 \text{ kcal/mol}$. Therefore, an SWNT with armchair chirality could form the most stable SWNT–GC system due to the distinct chiral angle.²⁷ Note that we have utilized armchair SWNT for our simulations due to its stronger interaction with GC.

The Influence of SWNT Length and GC Polymer Length on GC Wrapping Behavior

To understand the wrapping process of GC on SWNTs length, we have modeled armchair SWNT (6, 6) with lengths of 110.68, 140.19, and 169.71 \AA . Figure 8 shows the wrapping after 3.5 ns. It can be seen that all the wrappings are nearly same, which is in a mostly linear shape. However, the contact area is not the same, and this may affect overall interaction energy. We

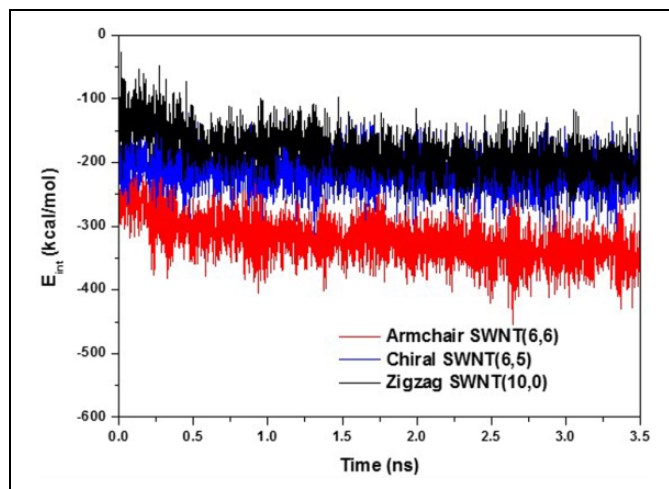


Figure 7. Interaction energies for SWNT–GC with different chiralities as a function of time. The chiral SWNT (6, 5), armchair SWNT (6, 6), and zigzag SWNT (10, 0) were used. GC polymers were 30 RU long. GC indicates glycated chitosan; RU, repeating unit; SWNT, single-walled carbon nanotube.

have also simulated for different RUs of GC (10, 20, and 50), which have similar wrapping patterns (data not shown).

Figure 9A displays interaction energy of GC with different lengths of SWNT, where average interaction is calculated to be

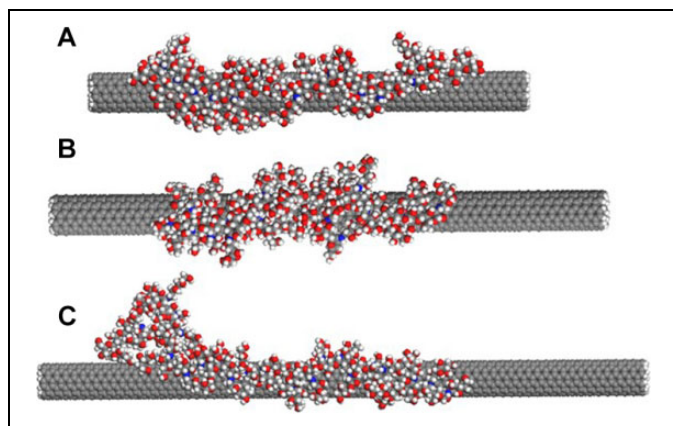


Figure 8. Simulation snapshots of GC wrapped around SWNT (6, 6) with lengths (A) 110.68, (B) 140.19, and (C) 169.71 Å. We kept same diameter (approximately 8 Å). GC polymers were 30. GC indicates glycosylated chitosan.

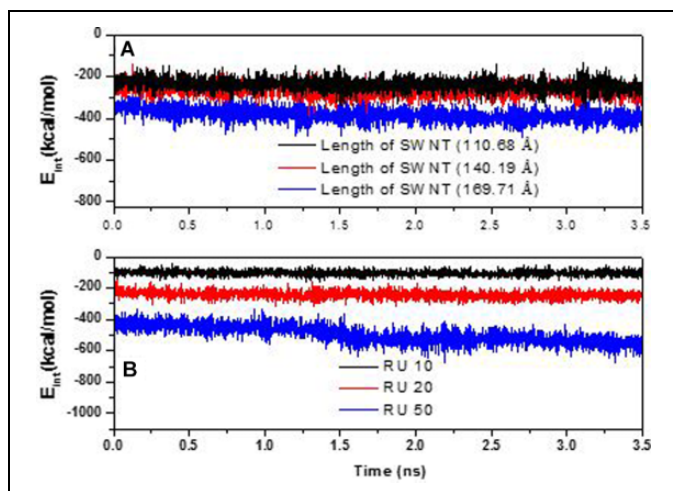


Figure 9. Interaction energies of GC: (A) with different lengths of SWNT, and (B) with RU of GC as a function of time. The armchair SWNT (6, 6) was used. GC indicates glycosylated chitosan; RU, repeating unit; SWNT, single-walled carbon nanotube.

−249.65 (33.32), −271.78 (30.26), and −394.22 (29.94) kcal/mol for SWNTs with length 110.68, 140.19, and 169.71 Å, respectively. Figure 9B shows the interaction energy for GC with 10, 20, and 50 RUs. The average interaction energies of 10, 20, and 50 RUs are −104.10 (16.13), −245.29 (19.84), and −549.94 (33.67) kcal/mol, respectively. As can be seen by the disparity in interaction energies, the number of RUs in the GC polymer has a great impact on the SWNT–GC binding. While the length of SWNT does seem to play a role in determining the interaction energy between SWNT and GC, it does not have a strong effect.

Radial Distribution Function

To evaluate the intermolecular interactions between the carbon (C) atoms of the SWNT and various atoms of the GC polymer,

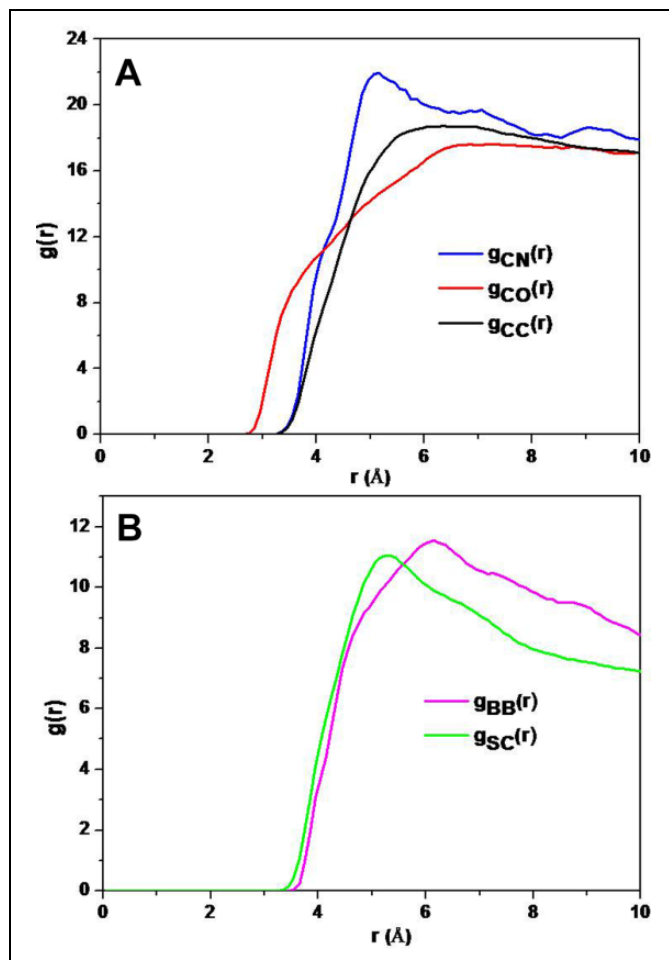


Figure 10. Radial distribution functions (RDFs) for the pairs of the carbon atoms of the SWNT and different atoms of GC. RDFs between the carbon atoms of the SWNT and the nitrogen, oxygen, and carbon atoms of GC were calculated. SWNT (12, 12) with a diameter of 16 Å and a GC polymer 30 RU were used. GC indicates glycosylated chitosan; RU, repeating unit; SWNT, single-walled carbon nanotube.

we calculated the radial distribution functions (RDFs), $g(r)$, of the various atoms of the GC polymer using the following equation:

$$g(r) = \frac{\rho(r)}{\rho}, \quad (5)$$

where $\rho(r)$ is the average number of atom pairs at a distance r and ρ is the overall density.³⁴ From Figure 10A, it can be seen that the first peaks oxygen (O) atoms, nitrogen (N) atoms, and carbon (C) are located at 3.5, 4.2, and 5.0 Å, respectively. This indicates that the O atoms of the GC polymer are closest to the SWNT followed by the N atoms and then the C atoms. These values (except for CC) are in good agreement with poly[2-(dimethylamino) ethyl methacrylate] DMAEMA-SWNT systems.³³ This suggests that GC is bound to SWNT by strong noncovalent interactions. Note that RDF values are remained same even when GC interacts with other types of SWNT. For further clarification, the RDF between C atoms in the backbone

(BB) of GC and SWNT as well as C atoms in the sidechain (SC) of GC and SWNT are calculated, which is shown in Figure 10B. The peaks are 5.25 and 6.25 Å for SC and BB, respectively. This result indicates that SC may affect how GC is wrapped around the SWNT surface.

Our MD simulations revealed that GC had different wrapping morphologies such as linear or helical type shape on the SWNT surface when it interacted with SWNT of different diameters, as shown in Figure 3. The radius of gyration of the GC molecule during the simulations shows that the GC molecule attained the smallest size when interacting with the SWNT(10,0). It was found that larger diameter of SWNT had higher interaction energy, as shown in Figure 5. This is due to the fact that the side chains of GC interacts with the SWNT more intensively as well as due to larger surface area of the SWNT.

The chirality of the SWNT also has significant bearing on the SWNT-GC binding based on interaction energy. The (6, 6) armchair SWNT had the highest interaction energy, and the (6, 5) chiral and (10, 0) zigzag SWNTs had lower interaction energies, as shown in Figure 7. This indicates that armchair SWNT has the capability to form the most stable SWNT-GC complex. However, SWNT chirality had significant impact on the wrapping behavior of the GC molecule.

An analysis of length of SWNT and RU of GC indicates that longer SWNT has higher interaction energy and RU of GC greatly affects binding characteristics, as shown in Figure 9. Furthermore, the length of SWNT has similar effect on the wrapping behavior of the GC molecule (Figure 10). From RDFs, we can assume that the noncarbon atoms of the GC polymer were closer to the SWNT than the carbon atoms. Besides, sidechain carbon atoms has greater influenced to the SWNT than the BB carbon atoms.

Discussion

In this study, an approach to determine the appropriate SWNTs and GC polymer to design an effective multifunctional SWNT-GC nanosystem for biomedical application is demonstrated using molecular dynamics simulation. Specifically, we used SWNTs of different chiralities, diameters, and lengths and GC of different RUs to investigate the binding characteristics of the SWNT-GC nanosystem. The limitations encountered in experimental studies when analyzing a functionalized SWNT system, specifically SWNT-GC, include the uncontrollable RU-length of GC polymer can be reduced by the computer simulations.

Based on our simulation, the stability of SWNT-GC increases with the length of GC. With respect to the SWNT chirality, SWNTs with armchair chirality had the highest SWNT-GC interaction energy. The SWNT-GC system becomes more stable with stronger interaction energy between the 2 molecules. Our results suggest that a long GC molecule conjugated to a large armchair SWNT would form the most stable SWNT-GC system. The understanding of the dynamic

structure of SWNT-GC will help improve the synthesis of SWNT-GC for biomedical applications.

Authors' Note

Leton Chandra Saha and Okhil Kumar Nag contributed to the work equally. Leton Chandra Saha is now affiliated with Institute of Fluid Science, Tohoku University, Sendai, Japan.

Declaration of Conflicting Interests

The author(s) declared no potential conflicts of interest with respect to the research, authorship, and/or publication of this article.

Funding

The author(s) disclosed receipt of the following financial support for the research, authorship, and/or publication of this article: This research was supported in part by grants from the US National Institutes of Health (RS20132225-106, R21 EB0155091-01, and R01 CA205348-01A1) and the Oklahoma Center for Advancement of Science and Technology (HR16-085).

ORCID iD

Wei R. Chen, PhD  <http://orcid.org/0000-0002-7133-5794>

References

1. Iijima S. Helical microtubules of graphitic carbon. *Nature*. 1991; 354(6348):56-58.
2. Bethune DS, Kiang CH, de Vries MS, et al. Cobalt-catalysed growth of carbon nanotubes with single-atomic-layer walls. *Nature*. 1993;363:605-607.
3. Baughman RH, Zakhidov AA, de Heer WA. Carbon nanotubes—the route toward applications. *Science*. 2002;297(5582):787-792.
4. Griswold RT, Henderson R, Goddard J, et al. Photothermal effects of immunologically modified carbon nanotubes. In: *Biophotonics and Immune Responses VIII*. Bellingham, WA: SPIE; 2013.
5. Bachilo SM, Balzano L, Herrera JE, Pompeo F, Resasco DE, Weisman RB. Narrow (n, m)-distribution of single-walled carbon nanotubes grown using a solid supported catalyst. *J Am Chem Soc*. 2003;125(37):11186-11187.
6. Kam NWS, Jessop TC, Wender PA, Dai H. Nanotube molecular transporters: internalization of carbon nanotube-protein conjugates into mammalian cells. *J Am Chem Soc*. 2004;126(22): 8650-8651.
7. Pantarotto D, Briand JP, Prato M, Bianco A. Translocation of bioactive peptides across cell membranes by carbon nanotubes. *Chem Commun*. 2004;(1):16-17.
8. Kostarelos K, Bianco A, Prato M. Promises, facts and challenges for carbon nanotubes in imaging and therapeutics. *Nat Nanotechnol*. 2009;4(10):627-633.
9. Kam KWS, Liu Z, Dai HJ. Functionalization of carbon nanotubes via cleavable disulfide bonds for efficient intracellular delivery of siRNA and potent gene silencing. *J Am Chem Soc*. 2005;127(36): 12492-12493.
10. Kam KWS, Liu Z, Dai HJ. Carbon nanotubes as intracellular transporters for proteins and DNA: an investigation of the uptake mechanism and pathway. *Angew Chem Int Ed Engl*. 2006;45(4): 577-581.

11. Liu Z, Cai W, He L, et al. In vivo biodistribution and highly efficient tumour targeting of carbon nanotubes in mice. *Nat Nanotechnol.* 2007;2(1):47-52.
12. Delogu LG, Venturelli E, Manetti R, et al. Ex vivo impact of functionalized carbon nanotubes on human immune cells. *Nanomedicine.* 2012;7(2):231-243.
13. Crescio C, Orecchioni M, Ménard-Moyon C, et al. Immunomodulatory properties of carbon nanotubes are able to compensate immune function dysregulation caused by microgravity conditions. *Nanoscale.* 2014;6(16):9599-9603.
14. Orecchioni M, Bedognetti D, Sgarrella F, Marincola FM, Bianco A, Delogu LG. Impact of carbon nanotubes and graphene on immune cells. *J Transl Med.* 2014;12:138.
15. Orecchioni M, Jasim DA, Pescatori M, et al. Molecular and genomic impact of large and small lateral dimension graphene oxide sheets on human immune cells from healthy donors. *Adv Healthc Mater.* 2016;5(2):276-287.
16. Ajayan PM, Schadler LS, Giannaris C, et al. Single-walled carbon nanotube-polymer composites: strength and weakness. *Adv Mater.* 2000;12(10):750-753.
17. Zhou F, Wu S, Song S, Chen WR, Resasco DE, Xing D. Antitumor immunologically modified carbon nanotubes for photothermal therapy. *Biomaterials.* 2012;33(11):3235-3242.
18. Zhou F, Song S, Chen WR, Xing D. Immunostimulatory properties of glycosylated chitosan. *J Xray Sci Technol.* 2011;19(2):285-292.
19. Chen WR, Carubelli R, Liu H, Nordquist RE. Laser immunotherapy: a novel treatment modality for metastatic tumors. *Mol Biotechnol.* 2003;25(1):37-43.
20. Song S, Zhou F, Nordquist RE, Carubelli R, Liu H, Chen WR. Glycosylated chitosan as a new non-toxic immunostimulant. *Immunopharmacol Immunotoxicol.* 2009;31(2):202-208.
21. Mori H, Hirai Y, Ogata S, Akita S, Nakayama Y. Chirality dependence of mechanical properties of single-walled carbon nanotubes under axial tensile strain. *Japanese J Appl Phys.* 2005;44(42):L1307-L1309.
22. Maehashi L, Ohno Y, Inoue K, Matsumoto K. Chirality selection of single-walled carbon nanotubes by laser resonance chirality selection method. *Appl Phys Lett.* 2004;85(6):858-860.
23. Minoia A, Chen L, Beljonne D, Lazzaroni R. Molecular modeling study of the structure and stability of polymer/carbon nanotube interfaces. *Polymer.* 2012;53(24):5480-5490.
24. Han Y, Elliott J. Molecular dynamics simulations of the elastic properties of polymer/carbon nanotube composites. *Comp Mat Sci.* 2007;39(2):315-323.
25. Liu W, Yang CL, Zhu YT, Wang MS. Interactions between single-walled carbon nanotubes and polyethylene/polypropylene/polystyrene/poly(phenylacetylene)/poly(p-phenylenevinylene) considering repeat unit arrangements and conformations: a molecular dynamics simulation study. *J Phys Chem C.* 2008;112(6):1803-1811.
26. Yang M, Koutsos V, Zaiser M. Interactions between polymers and carbon nanotubes: a molecular dynamics study. *J Phys Chem C.* 2005;109(20):10009-10014.
27. Xie J, Xue Q, Chen H, Keller A, Dong M. Different factors' effect on the SWNT-fluorocarbon resin interaction: a MD simulation study. *Computational Materials Science.* 2010;49:148-157.
28. Smith W, Yong CW, Rodger PM. DL_POLY: application to molecular simulation. *Mol Simul.* 2002;28(5):385-471.
29. Hoover WG. Canonical dynamics: equilibrium phase-space distributions. *Phys Rev A.* 1985;31(3):1695-1697.
30. Mayo SL, Olafson BD, Goddard WA III. DREIDING: a generic force field for molecular simulations. *J Phys Chem.* 1990;94(26):8897-8909.
31. Tsai JL, Tzeng SH, Chiu YT. Characterizing elastic properties of carbon nanotubes/polyimide nanocomposites using multi-scale simulation. *Composites Part B Eng.* 2010;41(1):106-115.
32. Tallury SS, Pasquinelli MA. Molecular dynamics simulations of polymers with stiff backbones interacting with single-walled carbon nanotubes. *J Phys Chem B.* 2010;114(29):9349-9355.
33. Saha LC, Mian SA, Jang J. Molecular dynamics simulation study on the carbon nanotube interacting with a polymer. *Bull Korean Chem Soc.* 2012;33(3):893-896.
34. Humphrey W, Dalke A, Schulten K. VMD: visual molecular dynamics. *J Mol Graph.* 1996;14(1):33-38.